J. Fluid Mech. (1975), *vol.* 70, *part* 3, *pp.* 529–542
Printed in Great Britain

Supercritical Reynolds number simulation for two-dimensional flow over circular cylinders

By EDMOND SZECHENYI

Office National d'Etudes et de Recherches Aérospatiales (ONERA),
92320 Châtillon, France

(Received 29 April 1974)

In wind-tunnel tests on bluff bodies the Reynolds number is often limited to values that are very much smaller than those of the flows being simulated. In such cases the experiments may have no practical significance whatsoever since both the fluctuating and the steady aerodynamic phenomena can vary considerably with Reynolds number.

This difficulty was encountered in an investigation of supercritical† incompressible flow over cylinders, and an attempt at artificially increasing the Reynolds number by means of surface roughness was made. In order to evaluate this simulation technique, the influence of various grades of surface roughness on the aerodynamic forces acting on cylinders of different diameters was studied over a wide range of Reynolds numbers in two very different wind tunnels. The results allow very positive conclusions to be drawn.

1. Introduction

Wind-tunnel tests on models often present problems of similarity and scale. These were encountered in an experimental investigation concerning the fluctuating aerodynamic forces acting on large bluff cylindrical bodies such as power-station chimneys subjected to wind. A good representation of the real conditions requires that the real Reynolds number be respected, but this becomes difficult for very large structures. For example, the dimensions of large chimneys and the possible wind speeds are such that the real Reynolds numbers are of the order of 20×10^6 while the upper limit in available wind tunnels is about 6×10^6 in quasi-incompressible flow with acceptable tunnel blockage (i.e. Mach number $\leqslant 0{\cdot}3$). Earlier experiments on smooth cylinders by Loiseau & Szechenyi (1972*a*, *b*) had shown that transitional (critical) flow exists at Reynolds numbers in the range 2×10^5 to 6×10^6, the flow beyond that being supercritical. Consequently in the wind tunnels existing in France it is impossible to conduct experiments on smooth cylinders in incompressible supercritical flow though this is in fact the flow that exists around real large structures.

It may be useful to recall that the flow regime in two-dimensional flow over

† In this paper the prefixes 'trans' and 'super' are used in the same order as in transonic and supersonic speeds; i.e. 'trans' comes before 'super'. This order is the reverse of that found in some well-known publications, but is used by a number of authors, e.g. Sachs (1972).

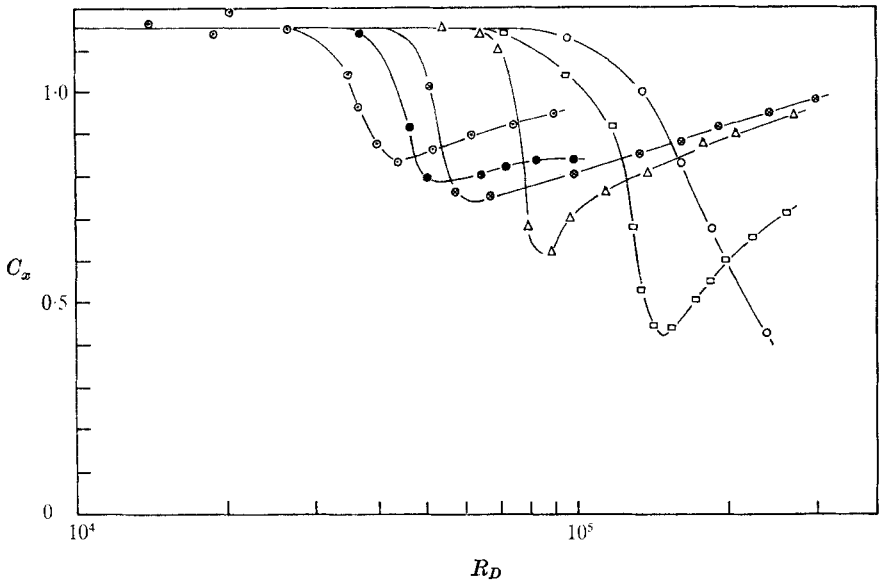

FIGURE 1. Fage & Warsap's results for the steady drag coefficient. ○, smooth cylinder; □, $\delta/D = 2 \times 10^{-3}$; △, $\delta/D = 4 \times 10^{-3}$; ⊗, $\delta/D = 7 \times 10^{-3}$; ●, $\delta/D = 9 \times 10^{-3}$; ⊙, $\delta/D = 2 \times 10^{-2}$.

a circular cylinder is a function of the boundary-layer flow in the vicinity of the point of separation on the cylinder. The character of this boundary layer depends on the Reynolds number and on the surface condition of the cylinder. The critical (or transcritical) regime is that in which the boundary layer changes from laminar to turbulent with increasing Reynolds number.

In the sub- and supercritical regimes, vortex shedding is periodic, resulting in an alternating circulation which generates fluctuating pressures with a well-defined frequency given by $f_s = S_s V/D$. (In this paper a subscript s on the frequency f or the Strouhal number S denotes its value for vortex shedding.) In transitional (or critical) flow separation is neither regular nor periodic and the resulting fluctuating pressures are random, giving a spectrum of high energy content over a frequency band stretching from near the steady-state value to an upper limit slightly beyond the shedding frequency in subcritical flow. Moreover the separation point in transcritical flow is far downstream from its position for the other two regimes; consequently the wake is narrower, resulting in a smaller steady drag force.

It is clear that the cylinder surface condition must have an important effect on the transition of the boundary layer and hence on the value of the Reynolds number at the onset of critical flow. Fage & Warsap (1930) demonstrated this by showing that the steep drop in the steady drag C_x† (characteristic of critical flow) occurs at progressively smaller Reynolds numbers with increasing surface roughness (figure 1).

† The international symbol C_x is used for the steady drag. The traditional symbols C_L and C_D for the lift and drag are retained for the unsteady force coefficients.

This fact has been used in the present study in an attempt to produce supercritical flows on cylinders by means of surface roughness (in the same manner as increased diameter, speed or flow density would do) with a view to investigating the fluctuating forces in this flow regime. However it must be pointed out that the effect of surface roughness on the steady drag does not prove that the fluctuating lift will be affected in the same way.

There is little published work concerning high Reynolds number simulation by means of surface roughness. However, Armitt's (1968) use of surface roughness on cooling-tower models should be mentioned. More recently Batham (1973) tackled the problem for circular cylinders but unfortunately was limited in his experiments to a Reynolds number of $2{\cdot}35 \times 10^5$, which is extremely restrictive, as subsequent results will show. However his results bear out the conclusions of this paper.

2. Experimental methods

2.1. *Wind tunnels and cylinders*

The experiments were conducted in the ONERA's S2-MA and S3-MA wind tunnels, which have working sections $1{\cdot}77 \times 1{\cdot}75$ m and $0{\cdot}78 \times 0{\cdot}56$ m respectively with perforated walls parallel to the cylinder axis. In both cases the cylinder spanned the tunnel section and was fixed rigidly to the tunnel walls. The test cylinder used in S2-MA had a diameter of 0·4 m, giving Reynolds numbers ranging from $2{\cdot}1 \times 10^5$ to $6{\cdot}5 \times 10^6$ with the maximum flow speed limited to 100 m/s in order not to move too far out of the incompressible regime. Three cylinders spanning the shorter dimension of the wind-tunnel section were tested in S3-MA. These had diameters of 0·14, 0·10 and 0·06 m, giving an overall Reynolds number range of $9{\cdot}6 \times 10^4$ to $4{\cdot}2 \times 10^6$. These dimensions give blockage ratios of 0·077, 0·128 and 0·179 for S3-MA and of 0·23 for S2-MA. The consistency of the results for the three cylinders in S3-MA shows that the wall perforations were sufficient to account for the largest tunnel blockage without the need for corrections. As far as S2-MA is concerned, preliminary experiments with cylinders of different diameters showed that blockage corrections were unnecessary for a blockage ratio of 0·23.

2.2. *Measuring techniques*

Measurement of unsteady lift force. As in previous experiments on smooth cylinders (see Loiseau & Szechenyi 1972*a*, *b*), the fluctuating lift force was measured by means of pressure transducers placed on the circumference of the cylinder in the same cross-sectional plane. The lift force was obtained through a real-time summation of the lift components of the pressure at each transducer.

The transducers were mounted 3 mm from the cylinder surface and were connected to it by pressure holes 1 mm in diameter. The transducers used (Kulite type CQL-080-5) have a natural frequency of 70 kHz and thus present no problems of varying frequency and phase response over the frequency range of interest (30–400 Hz).

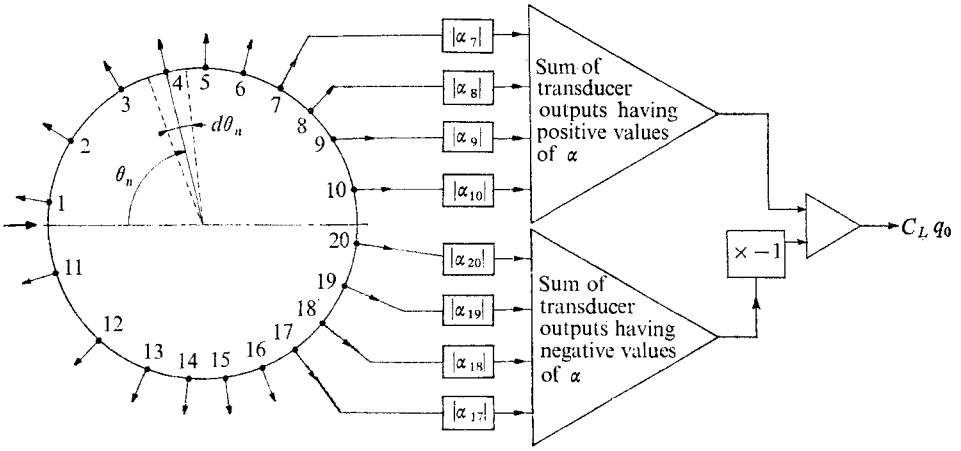

FIGURE 2. Positions of pressure transducers and diagram of the fluctuating lift measuring procedure.

Past experience had shown that twenty judiciously placed transducers could adequately represent the circumferential unsteady pressure variations. Figure 2 indicates these positions and illustrates the force measurement principle. The weighting coefficient α_n applied individually to the output signal of each transducer is a function of the position of that transducer and of the arc length over which it is assumed to measure the mean fluctuating pressure. The procedure can be represented by

$$\text{fluctuating lift coefficient} \equiv C_L = \sum_{n=1}^{20} \frac{p_n}{q_0} \alpha_n,$$

where p_n is the fluctuating pressure measured by transducer n, $q_0 = \frac{1}{2}\rho V^2$ and

$$\alpha_n = \sin(\tfrac{1}{2} d\theta_n) \sin\theta_n$$

(the meanings of the various terms in this expression are given in figure 2).

The cylinder tested in S2-MA was equipped with three force-measuring transducer sets whose axial positions were variable in order to permit spanwise correlations of the fluctuating lift forces.

Measurement of steady drag. The transducers used to measure the fluctuating lift force also gave the steady pressures. Summation of the appropriately weighted drag components of these pressures yielded the steady drag. As explained above, the transducers were positioned for best lift measurements and consequently were less well placed for drag measurements. This obviously led to a loss in accuracy.

2.3. *Surface roughness*

The cylinders' surfaces were roughened with calibrated spherical glass beads of seven different sizes, varying in diameter δ from 0·04 to 0·7 mm. These beads were stuck to the cylinder with a varnish by projecting in turn varnish and beads with spray guns in such a manner as to obtain a fairly uniform random distribution over the whole cylinder surface.

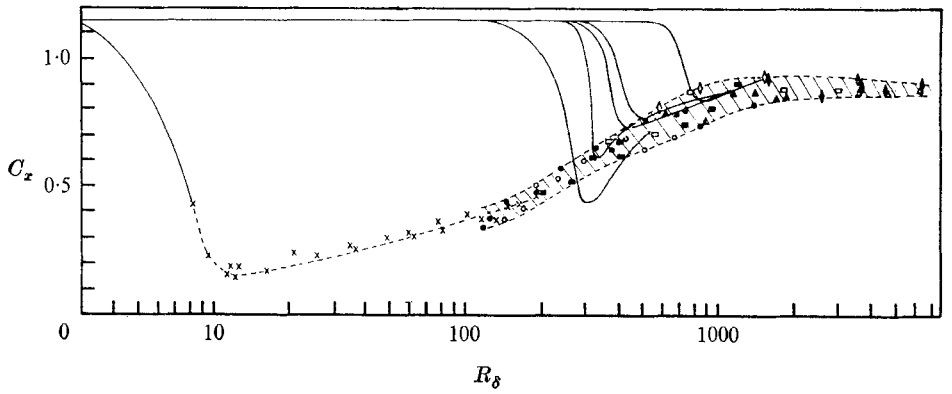

FIGURE 3. The steady drag coefficient. ——, results of Fage & Warsap (see figure 1). Results obtained for roughened cylinders: ○, $\delta/D = 1{\cdot}5 \times 10^{-4}$; ●, $\delta/D = 4 \times 10^{-4}$; ■, $\delta/D = 6{\cdot}7 \times 10^{-4}$; ▲, $\delta/D = 10^{-3}$; ◇, $\delta/D = 8 \times 10^{-4}$; △, $\delta/D = 1{\cdot}4 \times 10^{-3}$; □, $\delta/D = 1{\cdot}7 \times 10^{-3}$; ◆, $\delta/D = 2 \times 10^{-3}$. -- × --, smooth cylinder with R_δ calculated by assuming $\delta/D = 3{\cdot}5 \times 10^{-5}$.

3. Experimental results

3.1. *Steady drag*

An examination of all the drag results obtained (for all the various roughness sizes and all the cylinders) shows that for the larger roughness particles and the greater Reynolds numbers the steady drag coefficient C_x is no longer a function of cylinder diameter but of roughness particle diameter instead. Consequently the results are presented in terms of this parameter.

Figure 3 shows the results for C_x obtained here, as well as some obtained by Fage & Warsap, in terms of the Reynolds number R_δ *based on the roughness particle diameter.* (The Reynolds number based on the cylinder diameter is termed R_D.) Within broad limits of experimental error, the present results for the higher (supercritical) values of R_δ, as well as those due to Fage & Warsap, collapse onto a single curve.

If we now suppose that the presence of surface roughness is equivalent to an increase in the diametral Reynolds number R_D, the magnitude of this increase can be estimated by fitting the curve obtained for smooth cylinders (shown dashed in figure 3) onto the end of the mean curve in figure 3. Working back from the resulting values of R_δ on the abscissa, this procedure gives an effective relative roughness $\delta/D \approx 3{\cdot}5 \times 10^{-5}$ for *all* the smooth cylinders. Consequently the effective increase in diametral Reynolds number is by a factor of $\delta/3{\cdot}5 \times 10^{-5}D$ for a cylinder of diameter D and surface roughness diameter δ. The smooth-cylinder curve from Fage & Warsap (see figure 1) was also plotted in figure 3 after applying this effective roughness ratio. The agreement with present results is good.

It is also interesting to note the variation of C_x with respect to R_δ shown in figure 3. The drag increases with Reynolds number up to a value of about 1000 of this parameter and then remains constant at $C_x \approx 0{\cdot}9$.

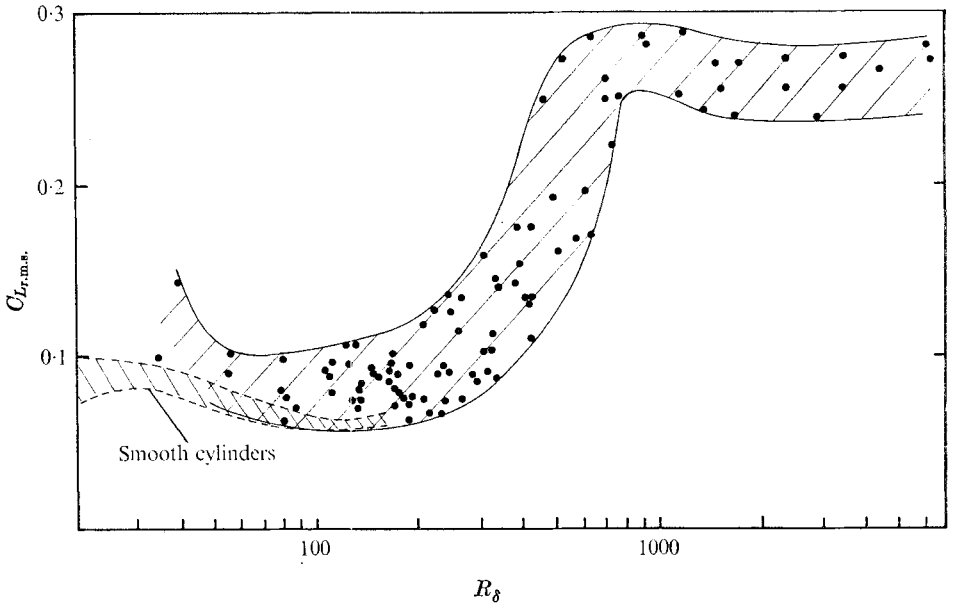

FIGURE 4. The r.m.s. overall fluctuating lift coefficient. R_δ for the smooth cylinder is calculated by assuming $\delta/D = 3{\cdot}5 \times 10^{-5}$. ●, experimental points from the roughened cylinders.

3.2. *Fluctuating lift*

Lift coefficient (r.m.s.). The envelope containing most of the lift coefficients measured on roughened cylinders is shown in figure 4, where the results are given in terms of the roughness Reynolds number R_δ. Plotting the results in terms of this parameter again gives a coherent representation. The envelope of the results for the unsteady lift measured on smooth cylinders was also plotted (dashed) in figure 4, by assuming the same effective surface roughness as for the steady drag (i.e. $\delta/D \approx 3{\cdot}5 \times 10^{-5}$). The graphical fit does not contradict the previous findings. The few lift-coefficient results falling outside the envelope of figure 4 were all measured on cylinders having very large surface roughnesses. It seems that in these cases vortex shedding is disturbed though the steady drag results show no abnormalities. A study of the lift spectra will give a clearer picture of this.

Lift spectra. The lift spectra are undoubtedly the most useful set of results because they provide the simplest criteria for classifying the flow regimes that produced them. The transcritical lift spectrum reveals a quasi-random pressure signal while the sub- and supercritical regimes are characterized by a clear and dominant peak at the shedding frequency. Typical examples are shown in figure 5.

When the ratio of roughness particle diameter to cylinder diameter exceeds a certain limiting value, the single well-defined peak at the shedding frequency breaks up and a more complicated spectral shape associated with a much reduced spectral level is formed (figure 6). This occurs in the cases for which the total lift coefficients no longer fall within the envelope of figure 4.

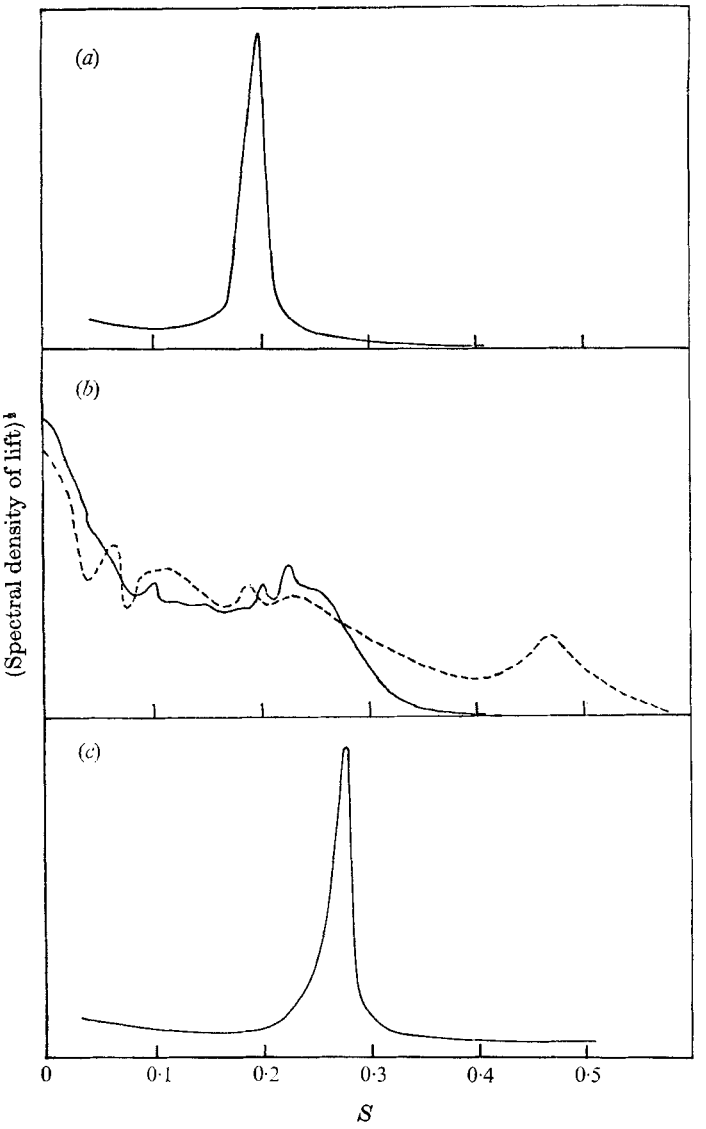

FIGURE 5. Typical fluctuating lift spectra for the three flow regimes. (*a*) Subcritical flow. (*b*) Transcritical flow, smooth cylinder: ——, $R_D = 3{\cdot}7 \times 10^6$; – – –, $R_D = 6{\cdot}3 \times 10^5$. (*c*) Supercritical flow.

Thus in these cases the roughness particles must be too large with respect to the cylinder diameter and destroy the regular shedding. The largest ratio δ/D still allowing periodic shedding has been determined only very approximately; it was found that for $\delta/D = 2{\cdot}2 \times 10^{-3}$ the lift forces were still harmonic while for $\delta/D = 2{\cdot}8 \times 10^{-3}$ the shedding was clearly disturbed (figure 6).

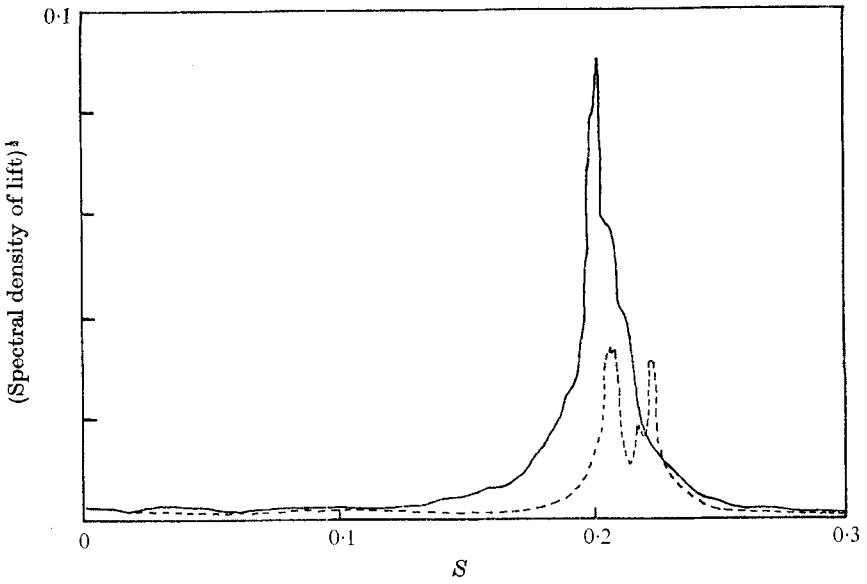

FIGURE 6. Fluctuating lift spectra for highly roughened cylinders. ——, $\delta/D = 2{\cdot}2 \times 10^{-3}$, $R_\delta = 6240$; ----, $\delta/D = 2{\cdot}8 \times 10^{-3}$, $R_\delta = 9200$.

3.3. *Reynolds numbers at transition between the flow regimes*

An inspection of the lift spectra produced by each roughness particle size for each cylinder at different Reynolds numbers yields the approximate Reynolds numbers at the limits of the flow regimes. Figure 7 summarizes these results.

By transforming the ordinate variable of figure 7 to the roughness Reynolds number R_δ (by multiplication of the ordinate variable by the abscissa variable) one obtains figure 8. This figure shows clearly that the change from transcritical to supercritical flow always occurs at a value of R_δ between 170 and 220. At first sight it would seem that the results obtained for smooth cylinders are in contradiction with the others. However, if one applies the effective roughness ratio referred to earlier (i.e. $\delta/D = 3{\cdot}5 \times 10^{-5}$), the change to the supercritical regime occurs at $R_\delta = 205$.

The limit of the ratio of roughness diameter to cylinder diameter is also shown in figure 8 and reveals that in order to generate a supercritical flow by means of surface roughness the diametral Reynolds number must have a value of at least 10^5. Consequently it appears that subject to this limit the roughness Reynolds number is the only parameter determining the change in the flow regime from trans- to supercritical, which implies that the absolute roughness dimension is the only governing size parameter.

The limit between the sub- and the transcritical regimes is much less sensitive to surface roughness. An extrapolation in figure 8 shows that it will probably not drop far below a diametral Reynolds number of 10^5 for roughness sizes that are acceptable from the point of view of periodic shedding.

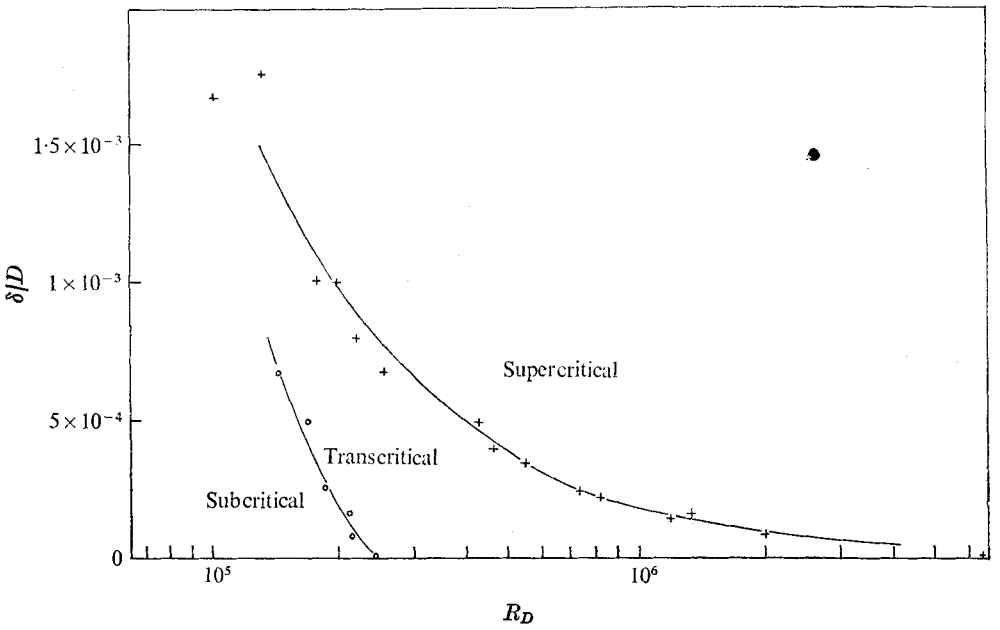

FIGURE 7. Limits of flow regimes for different ratios of roughness size to cylinder diameter. ○, sub- to transcritical; +, trans- to supercritical.

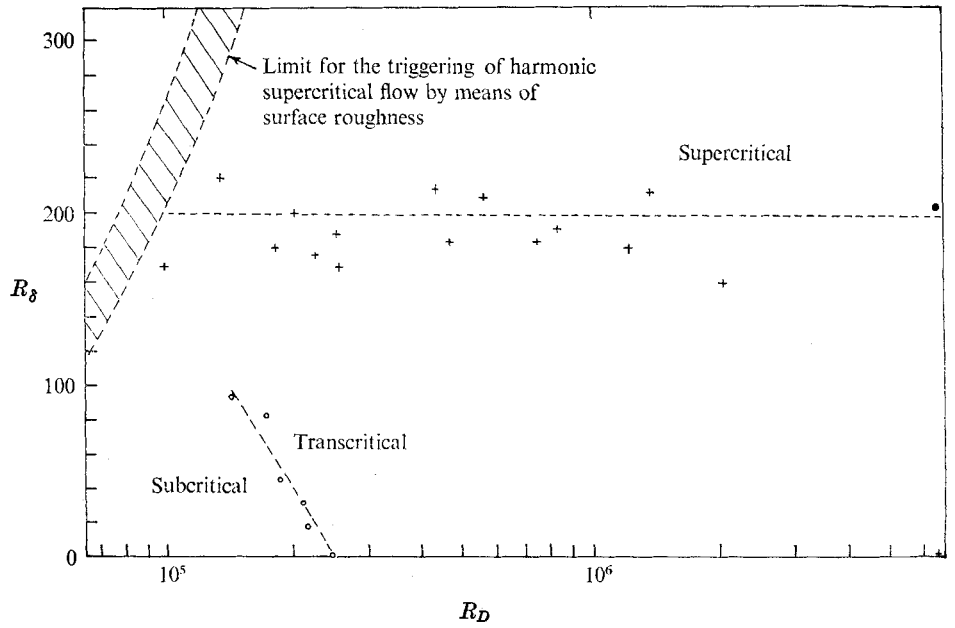

FIGURE 8. Limits of flow regimes in terms of the roughness Reynolds number. ●, sub- to transcritical; +, trans- to supercritical; ○, smooth cylinder when effective roughness $\delta/D = 3{\cdot}5\times10^{-5}$ is applied.

3.4. *Strouhal number*

The lift spectra permit an accurate assessment of the shedding frequency f_s, which leads to the shedding Strouhal number S_s. It is well known that S_s has a value of the order of 0·2 in subcritical flow. Roshko (1961) and Walshe (1972) have both shown that this parameter is larger in supercritical flow but its value remains ill defined owing to the lack of experiments at sufficiently high Reynolds numbers.

The quasi-random lift spectra of the critical regime show at most a weak shedding-frequency component, which is frequently insufficient to determine a value of S_s. When determinable, this value is of the same order as that for subcritical flow. The value $S_s \approx 0{\cdot}4$ (see figure 5) often found in publications dealing with critical flow has a different interpretation. Analysis of local pressure spectra (Loiseau & Szechenyi 1972*a*) shows that there is no shift in the normal shedding frequency and that the higher frequency phenomenon has a maximum pressure in the vicinity of the trailing edge of the cylinder. A possible explanation for this double-frequency lift force is that the pressures normally engendered at this double frequency near the trailing edge are no longer perfectly symmetrical with respect to the flow plane (as they are for regular vortex shedding), and thus their lift components do not cancel out.

The results for S_s obtained in S2-MA are shown in figure 9 in terms of R_δ. Again the roughness Reynolds number is the governing parameter. S_s has a value of about 0·22 in subcritical flow, rising to 0·30 at $R_\delta = 200$, then dropping slowly to 0·26 and stabilizing at $R_\delta = 1000$. The results obtained for smooth cylinders were also plotted in figure 9, using the effective roughness ($\delta/D = 3{\cdot}5 \times 10^{-5}$) to calculate their positions on the abscissa. Values of the roughness Reynolds number of 200 and 1000 have been encountered before. The first is the limit at which the periodic shedding of supercritical flow is established while the second corresponds to the lower limit of steady values of C_x (figure 3) and C_L (figure 4).

The variation of the shedding Strouhal number with the roughness Reynolds number is similar in the two wind tunnels used. However, the values of S_s are lower in S3-MA (for both smooth and roughened cylinders), where they vary from 0·16 in subcritical flow to 0·21 for the supercritical regime (compared with 0·22 and 0·26 in S2-MA). This is the only discrepancy between the results obtained in the two wind tunnels and remains unexplained. Various possible reasons for this discrepancy have been put forward: tunnel blockage, the aspect ratio of the cylinders (diameter/length), the ratio of the boundary-layer thickness to the cylinder diameter, errors in speed and/or frequency measurements and free-stream turbulence. It is improbable that the first three of these parameters had any influence since they vary with cylinder diameter and all three cylinders in S3-MA gave the same shedding Strouhal numbers. The frequency and flow-speed measurements were cross-checked. Any error in the latter would in any case have been obvious when normalizing the steady pressure distribution. The question of turbulence is more delicate. It is known that S3-MA has a much greater *axial* speed fluctuation ($\sim 4\,\%$, situated mainly in the frequency band 1–3 kHz) than S2-MA ($\sim 0{\cdot}3\,\%$, between 0 and 1 kHz). Could this be responsible for a 25% difference in Strouhal number?

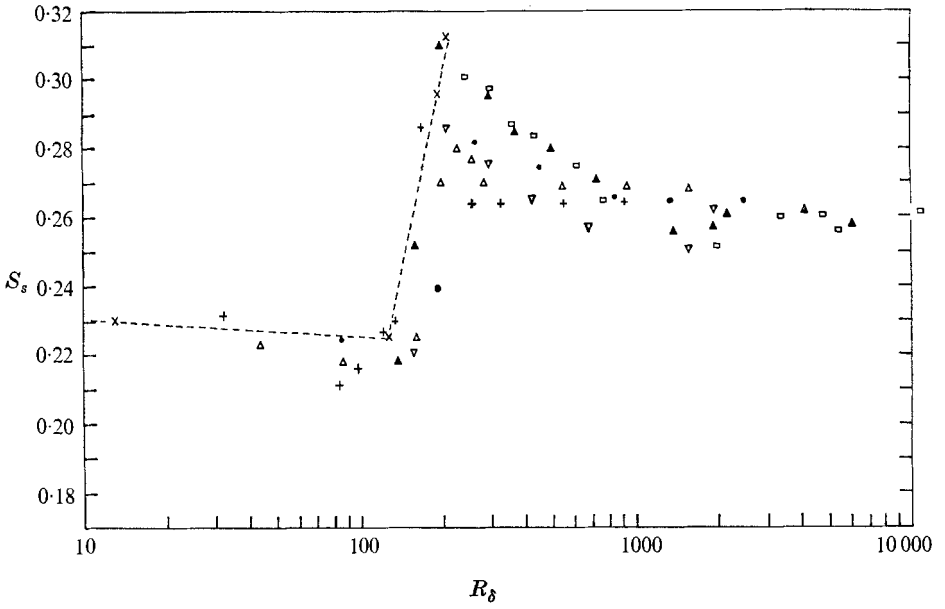

FIGURE 9. The shedding Strouhal number for various surface roughnesses. +, $\delta/D = 1{\cdot}5 \times 10^{-4}$; △, $\delta/D = 2{\cdot}5 \times 10^{-4}$; ●, $\delta/D = 5 \times 10^{-4}$; ▽, $\delta/D = 7{\cdot}5 \times 10^{-4}$; ▲, $\delta/D = 10^{-3}$; □, $\delta/D = 1{\cdot}75 \times 10^{-3}$; -- × --, smooth cylinder with R_δ calculated by assuming $\delta/D = 3{\cdot}5 \times 10^{-5}$.

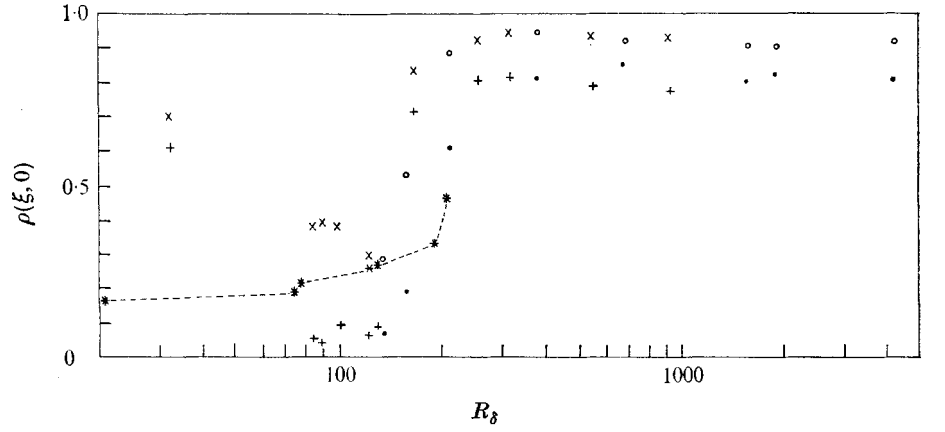

FIGURE 10. The cross-correlation coefficient of lift ($\tau = 0$). ×, $\delta/D = 1{\cdot}5 \times 10^{-4}$, $\xi = 1{\cdot}1$ diameters; +, $\delta/D = 1{\cdot}5 \times 10^{-4}$, $\xi = 2{\cdot}5$; ○, $\delta/D = 7{\cdot}5 \times 10^{-4}$, $\xi = 1{\cdot}1$; ●, $\delta/D = 7{\cdot}5 \times 10^{-4}$, $\xi = 2{\cdot}5$; -- × --, smooth cylinder with R_δ calculated by assuming $\delta/D = 3{\cdot}5 \times 10^{-5}$.

3.5. *The spanwise correlation*

Measurements for different surface roughnesses show that the spanwise correlation is independent of roughness size for any one flow regime, the roughness being instrumental only in establishing this regime. As an example, figure 10 shows the cross-correlation coefficient $\rho(\xi, \tau)$ at an incremental time $\tau = 0$ in terms of the roughness Reynolds number for two different roughness sizes and two spanwise

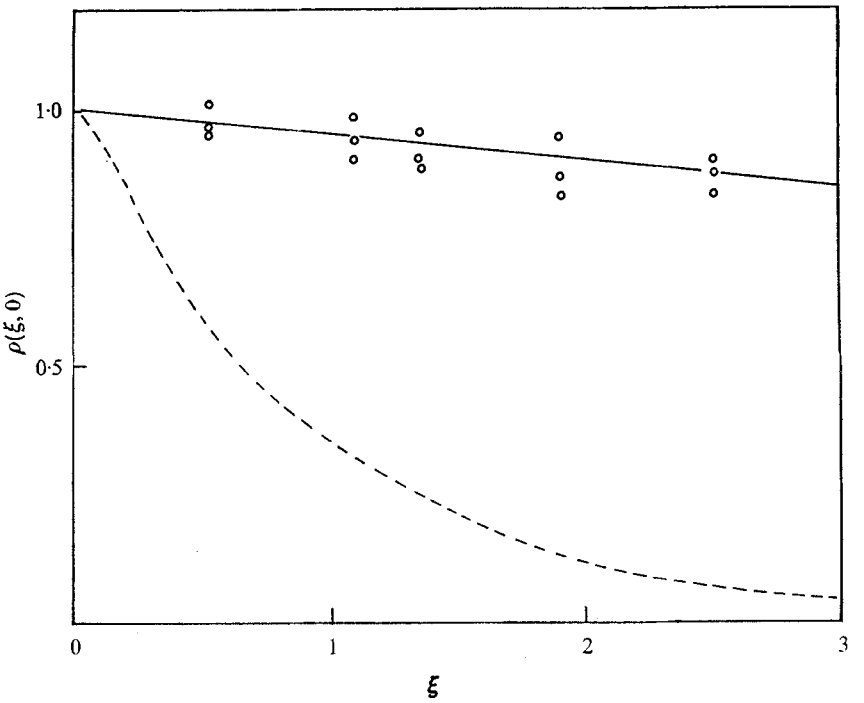

FIGURE 11. The spanwise cross-correlation of lift ($\tau = 0$). —○—, supercritical flow; ----, mean curve for transcritical flow.

spacings (ξ = spacing/D). The shape of the curve is the same for both roughness grades and reveals good correlation in subcritical flow then a drop that extends over the transcritical zone. At $R_\delta \approx 200$ the correlation rises sharply and becomes constant for increasing values of R_δ. The results obtained for smooth cylinders were plotted in the same figure after applying the effective roughness value to calculate the roughness Reynolds number for the abscissa.

Measurements in transcritical (smooth cylinder) and supercritical (roughened cylinder) flows were made for five spanwise spacings, giving the correlation curves in figure 11. The scatter of the results for transcritical flow was so great that for clarity only the mean curve is shown. Extrapolation of these results leads to correlation lengths

$$L = \int_0^\infty \rho(\xi, 0)\, d\xi$$

of one and at least nine diameters respectively for the transcritical and supercritical regimes.

3.6. *Flow visualization on the cylinder surface*

Flow-visualization tests were carried out for various roughness and diametral Reynolds numbers R_δ and R_D in such a way as to represent the various flow regimes in different ways. The results of these tests (summarized in table 1) corroborate the conclusions derived quantitatively.

Test	Test conditions δ/D	R_δ	R_D	Expected flow regime	Angular position of separation point	Remarks
1	0	0	$1{\cdot}5\times10^5$	Subcritical	74°	The position of the separation points does not vary along the length of the cylinder and corresponds to the results of other investigators, e.g. Achenbach (1968).
2	0	0	10^6	Transcritical	110–140°	There are two distinct separation points, whose positions vary considerably along the length of the cylinder. This double separation shows the existence of a separation bubble before the final turbulent separation.
3	$1{\cdot}5\times10^{-4}$	150	10^6	Transcritical	110–125°	Though the separation is axially more regular than in test 2, there is still some evidence of a separation bubble.
4	4×10^{-4}	400	10^6	Supercritical	95°	The separation point does not vary along the axis and has a characteristic value for supercritical flow (judging from results of Roshko 1961).
5	$1{\cdot}33\times10^{-3}$	4000	3×10^6	Supercritical	93°	Though the separation point seems to be slightly nearer the stagnation point than in test 4, the flow patterns look identical.

TABLE 1. The principal results of some of the surface flow-visualization tests

4. Conclusions

The results obtained in this study of two-dimensional flow over smooth and roughened cylinders all show that a change in flow regime takes place at a roughness Reynolds number of about 200 independently of the diametral Reynolds number. Since this limit separates the quasi-random transcritical flow from a flow domain whose measured parameters have the characteristics of the supercritical regime, it represents in all probability the conditions for which the surface boundary layer becomes turbulent at the point of flow separation. However, the separating boundary layer is probably not fully developed until the roughness Reynolds number reaches a value of about 1000, where the various parameters (C_x, C_L and S_s) become constant.

One can reasonably conclude that a correct surface roughness condition will provoke supercritical flow for $R_\delta > 200$. The condition that must be respected is $\delta/D < 2{\cdot}2 \times 10^{-3}$, which implies that $R_D \gtrsim 10^5$.

The results also show that a 'smooth' cylinder is not a special case but behaves as if it had a very small surface roughness. It seems that a cylinder whose natural surface roughness is very small will always be seen by a two-dimensional flow as having a roughness equivalent to the ratio $\delta/D \approx 3{\cdot}5 \times 10^{-5}$.

Finally, a note of caution. This high Reynolds number simulation depends entirely on the transformation of the separating boundary layer from laminar to turbulent. It is therefore applicable only in circumstances where the flow characteristics are entirely governed by this boundary layer, such as the two-dimensional flow considered in this investigation. If the aerodynamic forces are generated by a flow which is independent, or even partly independent, of the cylinder surface boundary layer, this principle cannot be applied. An important example of this is the case of an open-ended cylinder (chimney). Recent experiments have shown that the flow separation and vortex shedding from the free end govern the fluctuating force pattern over a portion of that end of the cylinder a number of diameters long.

REFERENCES

Achenbach, E. 1968 *J. Fluid Mech.* **34**, 625.

Armitt, J. 1968 *Proc. Symp. on Wind Effect on Buildings and Structures*, paper 6. Loughborough University.

Batham, J. 1973 *J. Fluid Mech.* **57**, 209.

Fage, A. & Warsap, J. E. 1930 *Aero. Res. Counc. R. & M.* no. 1283.

Loiseau, H. & Szechenyi, E. 1972*a* *Recherche Aérospatiale*, **5**, 279.

Loiseau, H. & Szechenyi, E. 1972*b* *IUTAM/IAHR Symp.* Springer.

Roshko, A. 1961 *J. Fluid Mech.* **10**, 334.

Sachs, P. 1972 *International Series of Monographs in Civil Engineering*, vol. 3, p. 62. Pergamon.

Walshe, D. E. J. 1972 Wind excited oscillations of structures. *Nat. Phys. Lab. Monograph.* H.M.S.O.